© 2021. Published by The Company of Biologists Ltd | Journal of Experimental Biology (2021) 224, jeb242409. doi:10.1242/jeb.242409

CORRECTION

Correction: The biomechanics of knuckle-walking: 3-D kinematics of the chimpanzee and macaque wrist, hand and fingers

Nathan E. Thompson

There was an error published in *Journal of Experimental Biology* (2020) **223**, jeb224360 (doi:10.1242/jeb.224360).

The description of the calculation of metacarpophalangeal (MCP) joint abduction and adduction was incorrect. It was originally described as the angle between the metacarpal and the projection of the phalangeal vector onto the plane of best fit of the metacarpals. This was not the case. The MCP adduction/abduction angle was calculated as the 3-D angle between the phalangeal vector projected onto the sagittal metacarpal plane (gray plane of Fig. 2) and the vector describing the actual position of the phalanges. The originally described calculation is sensitive to changes in MCP flexion and extension, whereas the calculation actually used is not. No data, analyses or conclusions are changed as a result of this; only the description of the calculation used in the Materials and Methods and the representation of this in Fig. 2 were incorrect.

The corrected text in Materials and Methods (third to last sentence in 'Metacarpophalangeal motion') reads: 'Adduction and abduction were calculated as the 3-D angle between the vector projection of the phalangeal markers onto the sagittal metacarpal plane (v_{pp_proj} in Fig. 2C,D) and the actual vector defining each phalanx. This calculation returns a value for abduction and adduction that is insensitive to the degree of MCP flexion and extension.'

The original and corrected versions of Fig. 2 are shown below. Both the online full-text and PDF versions of the article have been updated.

The authors apologise to the readers for any inconvenience caused and thank Dr Joris Leijnse for identification of this error.

Journal of Experimental Biology (2021) 224, jeb242409. doi:10.1242/jeb.242409

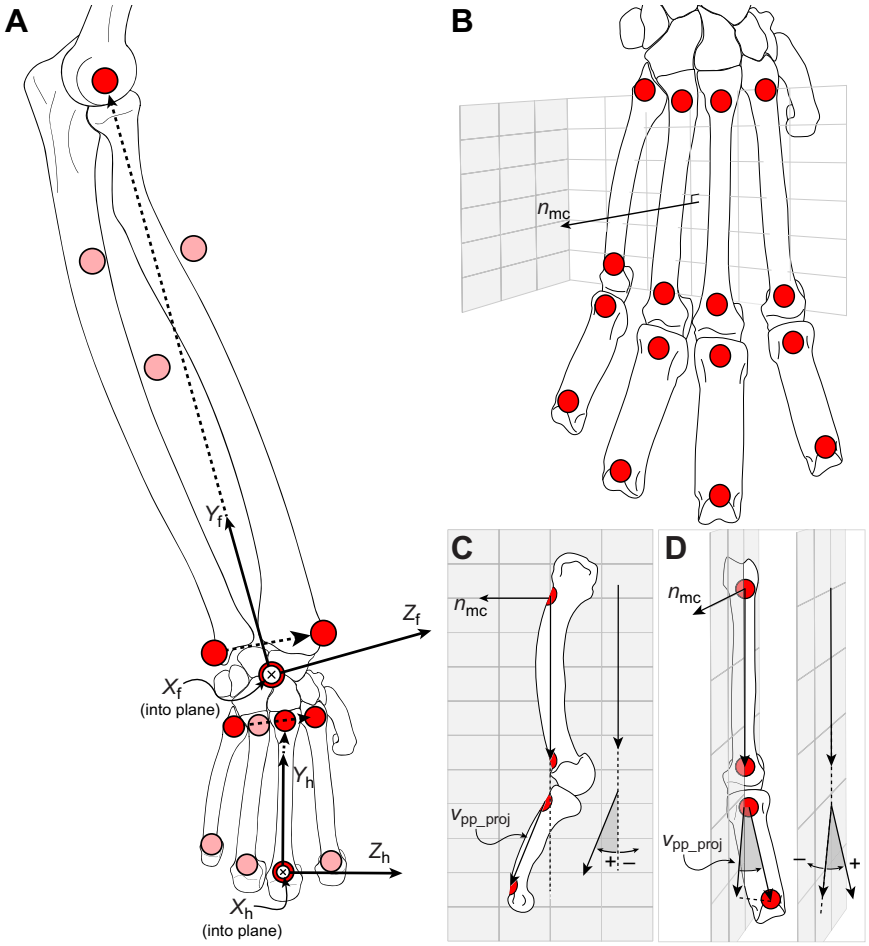

Fig. 2. (corrected). Forearm, hand and phalangeal coordinate systems and marker sets for the right side in dorsal view. Marker locations are described in Table S1. (A) The red markers are those that were used to define the forearm (X_f, Y_f and Z_f) or hand (X_h, Y_h and Z_h) coordinate system (black arrows). Dashed arrows represent vectors that were used to help orient the coordinate system. Pink markers are those additional markers that were used to help calculate wrist joint motion, but were not used in defining the coordinate system. (B) n_{mc} is the normal vector to a plane of best fit to all eight metacarpal landmarks (white plane; B). For each digit, a plane perpendicular to this, oriented along each metacarpal's base and head landmark, was used to describe the sagittal plane of each metacarpal (gray plane in B and C, describing sagittal plane of the second metacarpal). (C) The projection of the phalangeal vector onto this plane was used to describe flexion (–; deg) and extension (+; deg). (D) Adduction (–; deg) and abduction (+; deg) were calculated as the 3-D angle between the vector projection of the phalangeal markers (v_{pp_proj}) onto the sagittal metacarpal plane (gray plane) and the actual vector of the phalanges.

Journal of Experimental Biology (2021) 224, jeb242409. doi:10.1242/jeb.242409

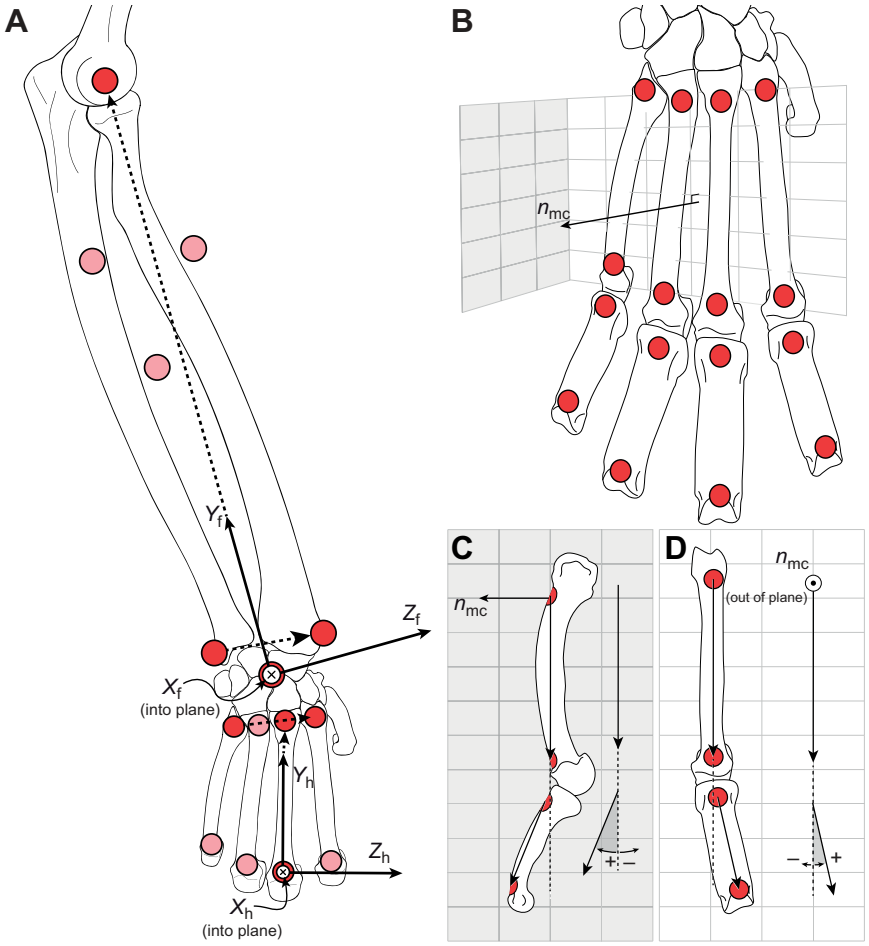

Fig. 2. (original). Forearm, hand and phalangeal coordinate systems and marker sets for the right side in dorsal view. Marker locations are described in Table S1. (A) The red markers are those that were used to define the forearm (X_f, Y_f and Z_f) or hand (X_h, Y_h and Z_h) coordinate system (black arrows). Dashed arrows represent vectors that were used to help orient the coordinate system. Pink markers are those additional markers that were used to help calculate wrist joint motion, but were not used in defining the coordinate system. (B) n_{mc} is the normal vector to a plane of best fit to all eight metacarpal landmarks (white plane; B). For each digit, a plane perpendicular to this, oriented along each metacarpal's base and head landmark, was used to describe the sagittal plane of each metacarpal (gray plane in B and C, describing sagittal plane of the second metacarpal). (C) The projection of the phalangeal vector onto this plane was used to describe flexion (–; deg) and extension (+; deg). (D) The projection of the phalangeal vectors onto the plane of best fit of the metacarpals was used to describe adduction (–; deg) and abduction (+; deg).

© 2020. Published by The Company of Biologists Ltd | Journal of Experimental Biology (2020) 223, jeb224360. doi:10.1242/jeb.224360

RESEARCH ARTICLE

The biomechanics of knuckle-walking: 3-D kinematics of the chimpanzee and macaque wrist, hand and fingers

Nathan E. Thompson*

ABSTRACT

The origin and evolution of knuckle-walking has long been a key focus in understanding African ape, including human, origins. Yet, despite numerous studies documenting morphological characteristics potentially associated with knuckle-walking, little quantitative three-dimensional (3-D) data exist of forelimb motion during knuckle-walking. Nor do any comparative 3-D data exist for hand postures used during quadrupedalism in monkeys. This lack of data has limited the testability of proposed adaptations for knuckle-walking in African apes. This study presents the first 3-D kinematic data of the wrist, hand and metacarpophalangeal joints during knuckle-walking in chimpanzees and in macaques using digitigrade and palmigrade hand postures. These results clarify the unique characteristics of, and commonalities between, knuckle-walking and digitigrady/palmigrady in multiple planes of motion. Notably, chimpanzees utilized more wrist ulnar deviation than any macaque hand posture. Maximum extension of the chimpanzee wrist was slight (5–20 deg) and generally overlapped with macaque digitigrady. Metacarpophalangeal joint motion displayed distinct differences between digits in both species, likely related to the timing of force application. These data also reveal that maximum metacarpophalangeal extension angles during knuckle-walking (26–59 deg) were generally higher than previously considered. In macaques, maximum metacarpophalangeal extension during digitigrady and palmigrady overlapped for most digits, highlighting additional complexity in the interpretation of skeletal features that may be related to limiting metacarpophalangeal motion. Most importantly, however, these new 3-D data serve as a fundamental dataset with which evaluation of proposed musculoskeletal adaptations for knuckle-walking can be tested.

KEY WORDS: Locomotion, Gait, Evolution, Ape, Quadrupedal

INTRODUCTION

Chimpanzees, bonobos and gorillas are unique among primates in their predominant use of knuckle-walking hand postures when terrestrial. Why, when and how many times this peculiar locomotor hand posture evolved has been the subject of intense scrutiny over the last 100 years in paleoanthropology (see the reviews of Begun, 2010; Crompton et al., 2008; Richmond et al., 2001 among others). Correspondingly, identification of skeletal correlates in the hands of apes reflecting knuckle-walking or other hand postures, has been the focus of an enormous amount of research within paleoanthropology (e.g. Richmond et al., 2001 and citations therein, and more recently Begun and Kivell, 2011; Kivell and Schmitt, 2009; Kivell et al., 2013; Lovejoy et al., 2009; Orr, 2005; Orr, 2016; Sayers et al., 2012; Simpson et al., 2018; Williams, 2010 among many others). Establishing and evaluating such form–function correlations requires not only robust extant morphological comparisons, but also specific locomotor data. Knowledge of bony motion, combined with force magnitudes, orientations and muscle activations are all crucial to drawing conclusions relating form to function. Yet remarkably little detailed quantitative biomechanical data on knuckle-walking exist from which such biomechanical inferences can be drawn. Without such data, the evaluation of musculoskeletal adaptations must necessarily rely on assumptions of knuckle-walking biomechanics.

Experimental studies of knuckle-walking largely began with the videographic studies by Tuttle (1967, 1969a,b, 1970). These, and a number of videographic studies since then, have documented qualitative and quantitative aspects of chimpanzee and gorilla knuckle-walking such as hand positioning (Doran, 1997; Jenkins and Fleagle, 1975; Thompson et al., 2018a) and frequency and variability with which individual digits contact the substrate (Inouye, 1994). More recently, the digital-level differences in force and pressure magnitude have also been documented via pressure pad studies (Matarazzo, 2013; Wunderlich and Jungers, 2009). Across the entire hand, the 3-D forces associated with knuckle-walking have been well documented (Demes et al., 1994; Kimura, 1985; Kimura et al., 1979; Li et al., 2004; Pontzer et al., 2014; Sockol et al., 2007; Thompson et al., 2018b). Yet, accurate kinematic data have remained scarce.

To date, the best kinematic data of the wrist and hand during knuckle-walking are from the cineradiographic study of Jenkins and Fleagle (1975). Their study illustrated a number of now classic kinematic characteristics of the chimpanzee proximal carpal and midcarpal joints. For instance, Jenkins and Fleagle (1975) demonstrated the close-packed position between the distal dorsal radius and concave portion of the scaphoid and highlighted the extension-limiting non-articular ridge on the dorsal scaphoid (Jenkins and Fleagle, 1975). They also qualitatively described wrist motion, both at the proximal and midcarpal joints, and established the relative contribution of these joints to flexion/extension and radial/ulnar deviation (Jenkins and Fleagle, 1975).

The study of Jenkins and Fleagle (1975) was groundbreaking and continues to be the chief source of kinematic information on chimpanzee knuckle-walking. But, despite the importance of those data, it was 2-D in nature. Owing to inherent limitations with 2-D kinematic methodologies, much data on joint and segment positions and ranges of motion over stance phase were only broadly characterized or remained unquantified. More recent 2-D studies have also documented wrist joint motion in chimpanzees (Finestone et al., 2018; Pontzer et al., 2014) and gorillas (Finestone et al., 2018). Two-dimensional studies, however, are inherently limited in documenting joint motion as the forearm and hand are known to

Department of Anatomy, NYIT College of Osteopathic Medicine, Old Westbury, NY 11568, USA.

*Author for correspondence (nthomp03@nyit.edu)

N.E.T., 0000-0002-9273-3636

Received 27 February 2020; Accepted 5 June 2020

Journal of Experimental Biology (2020) 223, jeb224360. doi:10.1242/jeb.224360

rotate out of plane relative to the direction of motion during knuckle-walking (Matarazzo, 2013; Tuttle, 1967; Wunderlich and Jungers, 2009). No study thus far has documented 3-D wrist or digit-level joint motion.

The lack of accurate, 3-D data on knuckle-walking has become particularly apparent in the light of an increasing numbers of studies correlating knuckle-walking with internal hand and wrist bone morphology. Such studies often make predictions that require knowledge of bone and force orientations (Barak et al., 2017; Chirchir et al., 2017; Dunmore et al., 2019; Lazenby et al., 2011; Macho et al., 2010; Matarazzo, 2015; Patel and Carlson, 2007; Tsegai et al., 2013; Zeininger et al., 2011). Without kinematic data, they remain assumptions. Indeed, such is the dearth of data that a recent study utilized bony morphology to hypothesize kinematic differences in wrist and metacarpophalangeal joint angles between chimpanzees and gorillas (Kivell and Schmitt, 2009). This hypothetical postural difference has since been relatively well adopted within the literature, and has subsequently been upheld as kinematic evidence of fundamentally different forms of knuckle-walking (Le Maître et al., 2017; Macho et al., 2010; Saunders et al., 2016; Schilling et al., 2014; Simpson et al., 2018; Thorpe et al., 2014). The adopting of hypotheses of extant kinematics based on morphology alone illustrates the challenges for functional morphologists when crucial, experimentally derived data on locomotion in extant apes are lacking.

Here, I present the first 3-D marker-based kinematic data on wrist and hand as well as digit-level metacarpophalangeal joint motion during knuckle-walking in chimpanzees, and during digitigrade, semi-digitigrade and palmigrade walking in rhesus macaques. These data form the first comprehensive 3-D kinematic dataset of hand postures during locomotion, and highlight unique kinematic aspects of chimpanzee knuckle-walking, as well as some commonalities between knuckle-walking and macaque digitigrady/palmigrady.

MATERIALS AND METHODS

Experimental subjects

Kinematic data were collected on two subadult male chimpanzees, *Pan troglodytes* (Blummenbach 1775), during knuckle-walking and two adult female rhesus macaques, *Macaca mulatta* (Zimmermann 1780), during quadrupedal digitigrady/palmigrady (chimpanzees: 8.7±0.2 years old, 51.5±2.9 kg; macaques: 5.2±0 years old, 5.1±0 kg). Chimpanzee data were collected at the Stony Brook University Primate Locomotion Laboratory and macaque data were collected at Northeast Ohio Medical University. All experiments were approved by the Institutional Animal Care and Use Committees at their respective institutions. Both species walked on a runway either of their own accord or following enticement with food rewards. Walking speeds were self-selected by the subjects and calculated *post hoc* using the linear distance traveled by a single acromion marker (or another marker near the shoulder if the acromion was not in view for the whole stride). To facilitate comparisons between species of different body sizes at different speeds, dimensionless speed $[v(\boldsymbol{g}l)^{-0.5}]$ and Froude number $[v^2(\boldsymbol{g}l)^{-1}]$ were calculated for all trials, where v is speed, $\boldsymbol{g}$ is gravitational acceleration (9.81 m s^{-2}) and l is effective forelimb length (Alexander and Jayes, 1983). Effective forelimb length was measured as the vertical distance between the acromion and a marker on the third proximal phalangeal head at midstance (the moment when the acromion was vertically positioned above the hand).

Kinematic methods

All kinematic data were recorded using a four-camera Xcitex motion capture system (Xcitex, Inc., Woburn, MA, USA) recording at 150 Hz, and largely followed methodologies published elsewhere (O'Neill et al., 2015; Thompson et al., 2015, 2018b,c). Six trials were collected for each subject, for a total of 12 trials for each species. Chimpanzees typically over-stride (the hand contacts the ground either at or further anteriorly than the foot). Because of this, all chimpanzee strides analyzed were 'outside' strides (e.g. Wunderlich and Jungers, 2009), where the hand was lateral to the foot at touchdown. This was unavoidable as otherwise the hand markers would be blocked by the foot and hind limb. To track motion, the fur on each subject was shaved and high-contrast markers were painted on the skin overlying palpable anatomical landmarks (Fig. 1, Movies 1, 2). Marker positions were tracked in the program ProAnalyst (Xcitex, Inc.) and raw x, y and z coordinates were exported for further analysis in MATLAB (The MathWorks, Inc., Natick, MA, USA). Each marker x, y and z component was filtered using a fourth-order, zero-lag low-pass Butterworth filter with a cut-off frequency of 9 Hz. After calculation of joint motion, all kinematic variables were truncated and normalized from 0 to 100% of stance phase.

The marker set utilized here allowed for calculation of 3-D motion of the wrist, 3-D positioning of the hand, as well as calculation of metacarpophalangeal joint motion in flexion/extension and abduction/adduction (Table S1, Fig. 2).

Wrist joint coordinate system

In order to calculate 3-D motion of the wrist, an anatomical marker set and coordinate system definitions were utilized that largely followed the recommendations set forth by the International Society

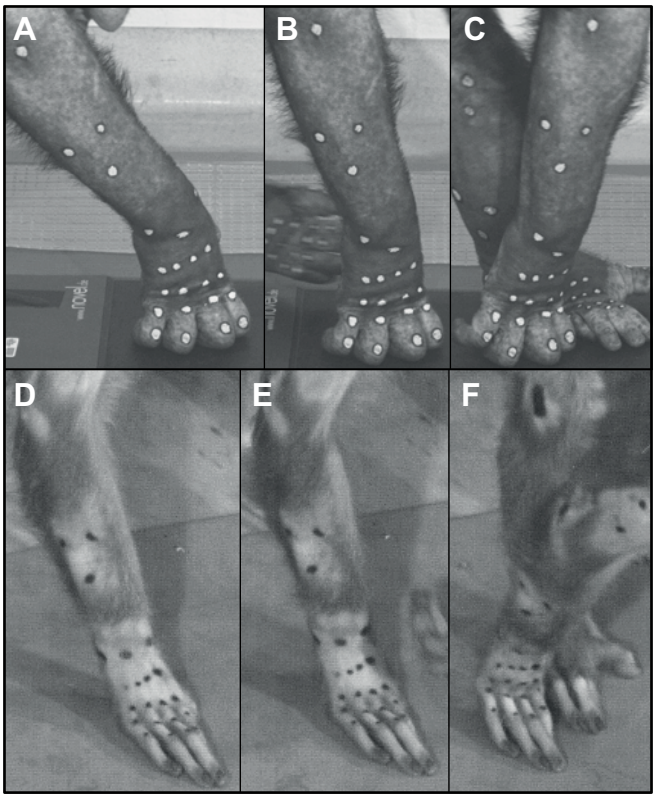

Fig. 1. Still frames of forelimb stance phase for chimpanzee knuckle-walking and macaque digitigrady. (A–C) Chimpanzees; (D–F) macaques. Images represent approximately 20% (A,D), 50% (B,E) and 85% (C,F) of the stance phase.

Journal of Experimental Biology (2020) 223, jeb224360. doi:10.1242/jeb.224360

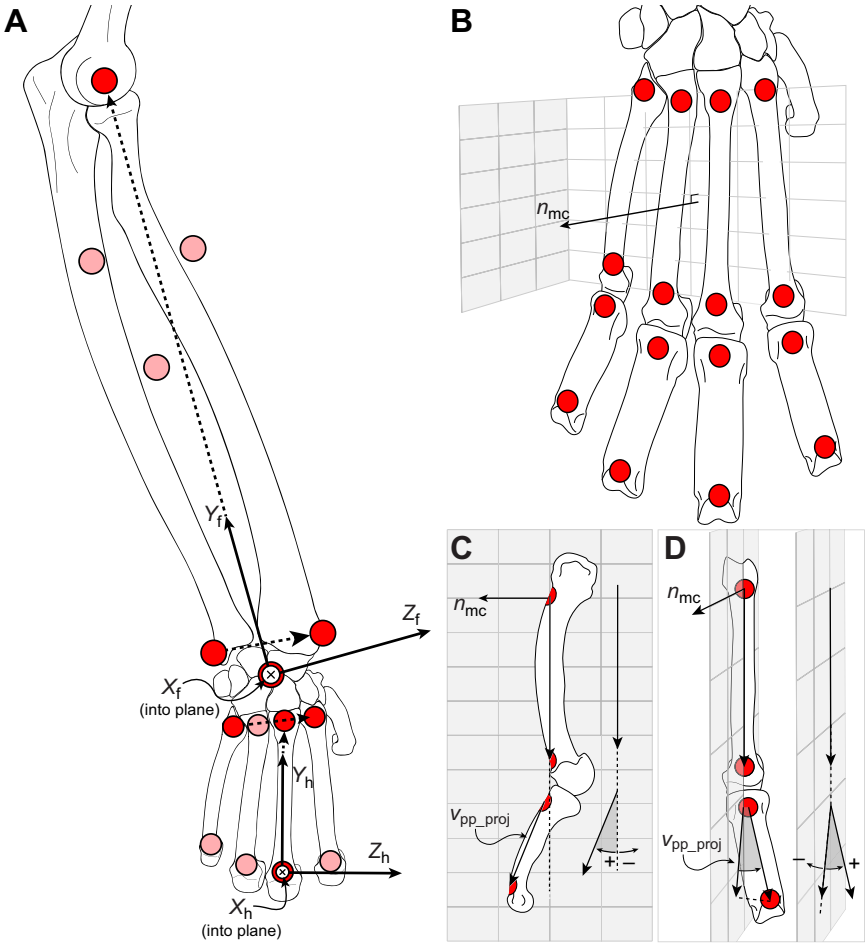

Fig. 2. Forearm, hand and phalangeal coordinate systems and marker sets for the right side in dorsal view. Marker locations are described in Table S1. (A) The red markers are those that were used to define the forearm (X_f, Y_f and Z_f) or hand (X_h, Y_h and Z_h) coordinate system (black arrows). Dashed arrows represent vectors that were used to help orient the coordinate system. Pink markers are those additional markers that were used to help calculate wrist joint motion, but were not used in defining the coordinate system. (B) n_{mc} is the normal vector to a plane of best fit to all eight metacarpal landmarks (white plane; B). For each digit, a plane perpendicular to this, oriented along each metacarpal's base and head landmark, was used to describe the sagittal plane of each metacarpal (gray plane in B and C, describing sagittal plane of the second metacarpal). (C) The projection of the phalangeal vector onto this plane was used to describe flexion (–; deg) and extension (+; deg). (D) Adduction (–; deg) and abduction (+; deg) were calculated as the 3-D angle between the vector projection of the phalangeal markers (v_{pp_proj}) onto the sagittal metacarpal plane (gray plane) and the actual vector of the phalanges.

for Biomechanics (ISB) for humans (Wu et al., 2005), albeit with some modifications.

The forearm coordinate system was defined such that for a right forearm: $+Y_f$ is directed proximally, on a line from a dorsal wrist landmark (forearm origin) to the lateral humeral epicondyle (Fig. 2). The $+X_f$ axis is defined as perpendicular to the Y_f axis, with positive pointing anteriorly (palmarly). This was calculated as the cross product of the $+Y_f$ unit vector and a unit vector on the line connecting the ulnar styloid process landmark to the radial styloid process landmark. The $+Z_f$ axis is perpendicular to X_f and Y_f and thus defines the mediolateral axis. Positive Z_f is directed laterally (radially) from the dorsal wrist landmark. As per ISB conventions, to maintain the correct sign conventions, for a left forearm $+Y_f$ is directed distally and $+Z_f$ is directed medially (ulnarly).

For calculation of wrist motion, the hand and metacarpal (MC) coordinate system was defined such that for a right hand, $+Y_h$ is directed proximally, from the MC3 head landmark (MC segment origin) along a line running through the MC3 head and base landmarks. The $+X_h$ axis is defined as perpendicular to the Y_h axis, with positive pointing palmarly. This was calculated as the cross product of the $+Y_h$ unit vector and a unit vector on the line connecting the fifth to the second metacarpal (MC) base landmarks. The $+Z_h$ axis is perpendicular to X_h and Y_h and thus defines the mediolateral axis. Positive Z_h is directed laterally (radially) from the MC3 base landmark. For a left hand, $+Y_h$ is directed distally and $+Z_h$ is directed medially.

Following the ISB recommendations, joint angles were calculated using Cardan angles and a *Z*, *X*, *Y* order of rotations. The neutral position was set such that the *Y*-axes of both segments were vertically aligned, and the *Z*- and *X*-axes parallel. This coordinate system was used to resolve wrist flexion/extension, ulnar/radial deviation and pronation/supination. It is important to emphasize, however, that the motion reported encompasses all of the joints between the forearm and metacarpals (radiocarpal joints, midcarpal joints and carpometacarpal joints), as is standard in the ISB recommendations (Wu et al., 2005). This also means that pronation/supination refers solely to motion between the forearm and wrist, and not to pronation/supination of the forearm itself. Joint angles were calculated using all eight of the metacarpal landmarks and all forearm markers that were present for more than ∼65% of the stride (always either six or seven markers).

Metacarpophalangeal motion

Metacarpophalangeal (MCP) flexion/extension and abduction/adduction were calculated by first using a principal components analysis to calculate a plane of best fit to all eight of the MC landmarks (white plane of Fig. 2B,D). The normal vector of this MC plane (n_{mc} in Fig. 2B) and the vector connecting the MC head and base landmarks for each digit then defined a plane perpendicular to the MC plane, oriented along each metacarpal (e.g. gray plane of Fig. 2B,C). Extension and flexion were calculated using the projection of the vector containing phalangeal head and base landmarks onto this plane. Extension and flexion were represented by positive and negative angles, respectively

Journal of Experimental Biology (2020) 223, jeb224360. doi:10.1242/jeb.224360

(Fig. 2C). Adduction and abduction were calculated as the 3-D angle between the vector projection of the phalangeal markers onto the sagittal metacarpal plane (v_{pp_proj} in Fig. 2C,D) and the actual vector defining each phalanx. This calculation returns a value for abduction and adduction that is insensitive to the degree of MCP flexion and extension. For all digits, abduction (motion away from the third digit) was positive and adduction (motion towards the third digit) was negative. For the third digit, abduction towards the second digit (radial deviation) was positive, and abduction towards the fourth digit (ulnar deviation) was negative.

Hand orientation

Hand orientation was assessed via the positioning of the orientation of the MC plane in the global coordinate system (fore–aft, mediolateral and vertical axes as defined by the runway). The MC normal vector (n_{mc} as defined above) was negated such that the vector pointed palmarly away from the MC plane. Strides that were analyzed for the left hand were flipped, such that all vectors could be visualized on the right side (Fig. 3A). The position of the $-n_{mc}$ vector was then projected onto the coronal plane and the coronal palm angle (PA_c) of this projection at touchdown and 50% of stance phased was recorded (Fig. 3B). The angle PA_c was 0 deg for a palm that was facing directly medially, and +90 deg for a palm that was directly posteriorly (Fig. 3B). The projection of the $-n_{mc}$ vector in the sagittal plane was recorded as sagittal palm angle (PA_s) at touchdown and 50% of stance phase (Fig. 3C). This angle was 0 deg when the palm was perpendicular to the ground, and +90 deg when oriented parallel to the ground (Fig. 3C). The endpoint of the $-n_{mc}$ vector was also plotted over the entire stance phase in 3-D. The pathway created by these endpoints was then projected onto the coronal and sagittal plane, such that the orientation of the hand can be visualized over the entire stance phase.

Data reporting

One of the largest limitations of the current dataset is dropped data. Given inherent limitations with camera positioning during data collection, for most trials, hand and forearm landmarks at some point rotated out of view, particularly late during stance phase. In some instances this affected only individual segments (e.g. one of four digital points), and caused truncation of one joint angle. In other cases, the loss of a single marker required the truncation of multiple segments (e.g. loss of a metacarpal marker). In the case of the forearm, the specific number of landmarks used to calculate motion was selected in order to maximize data resolution over the stride (though either six or seven markers were always used). Regardless, for the kinematic results, many trials do not possess data on some variables for the full range of stance phase. Because of this, data reporting differs slightly depending on the specific variable. For instance, it was not possible to report maximum, minimum and ranges of motion for all variables for all strides, as the data truncated before a minimum or maximum value was reached. Therefore, the number of strides used to calculate each specific variable is not the same and is reported on a case-by-case basis in the tables. In the text, *n*-values are reported when the number of strides is not the complete sample number (i.e. not six strides per individual, 12 total for chimpanzees and macaques). In addition, in some cases, motion was reported at specific times (e.g. touchdown or 50% of stance phase), or maximum and minimum values within a specified period of the stance phase were reported. Finally, because some trials truncated earlier than others, for all plots the individual trials are shown, rather than means and standard deviations.

In addition, one macaque subject only walked digitigrade (n=6 strides), while the other subject used either palmigrady (n=4 strides) or semi-digitigrady (n=2 strides). Semi-digitigrady herein refers to a hand position where the palm is only slightly elevated off of the ground. Because of this, for some data, where hand posture did not appear to influence the variable under consideration, the two macaque subjects are averaged together. In other cases, macaque data are reported by hand posture. When reporting data on semi-digitigrady within the text, the range of the two strides is often reported, rather than the mean plus or minus the standard deviation, in order to represent the data most faithfully.

Finally, one chimpanzee subject regularly held digits two and five off of the ground when knuckle-walking. These trials are displayed in the figures, but are excluded from the summary statistics in the tables and in the text. Following previous standards in reporting chimpanzee kinematic data (O'Neill et al., 2015) as well as the recommendations of Smith (2018), significance levels and *P*-values were not reported; rather, differences reported focus on the magnitude of the effect.

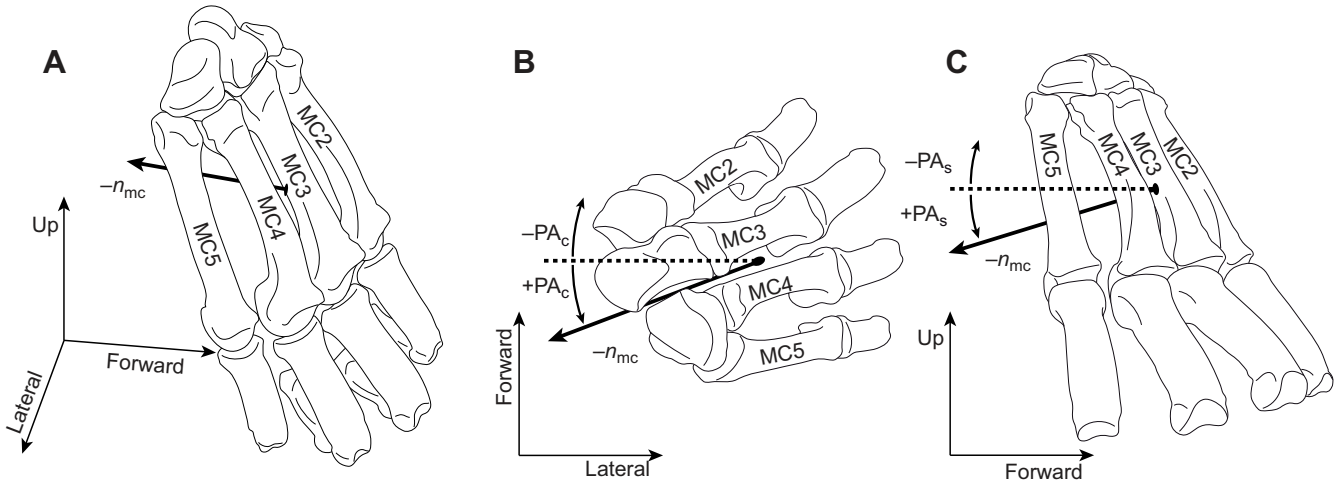

Fig. 3. Hand orientation coordinate system for the right hand. (A) The normal vector describing a plane fit to all eight metacarpal points was projected palmarly ($-n_{mc}$) in the global coordinate system (up, lateral and forward). The coronal palm angle, PA_c (B), and sagittal palm angle, PA_s (C), were recorded at touchdown and 50% of stance phase. The end point of the $-n_{mc}$ vector throughout stance phase was also plotted to visualize the change in orientation of the $-n_{mc}$ over stance phase.

Journal of Experimental Biology (2020) 223, jeb224360. doi:10.1242/jeb.224360

RESULTS

Walking speeds

Absolute walking speeds for the chimpanzee subjects were similar, though slightly faster, than for the macaque subjects (chimpanzees: 0.84±0.19 m s^{-1}; macaques: 0.79±0.09 m s^{-1}). Given the smaller body size of macaques, dimensionless speeds were nearly 45% greater in macaques (dimensionless speed, chimpanzees: 0.34±0.08; macaques: 0.49±0.05). One macaque subject utilized solely digitigrade hand postures, while the other utilized a mix of palmigrade (n=4) or semi-digitigrade (n=2) hand postures. This difference in hand-use preference was not explained by speed, which was nearly the same across all hand postures (dimensionless speed, digitigrade: 0.27±0.01; palmigrade, 0.26±0.00; semi-digitigrade, 0.26–0.27).

Wrist motion

Radial deviation

During knuckle-walking, chimpanzees generally touched down with a wrist that was ulnarly deviated (Fig. 4A; Table 1). Further ulnar deviation occurred during the first 10–20% of the stance phase. The wrist then gradually radially deviated throughout most of stance phase (20–80%), though it was generally still in an overall position of ulnar deviation. The wrist then quickly underwent ulnar deviation in preparation for swing phase.

The macaque pattern of wrist motion was somewhat similar to that of the chimpanzees. The wrist ulnarly deviated slightly in the first 20% of stance phase following touchdown, gradually radially deviated throughout stance phase, and finally began to ulnarly deviate again late in stance phase. However, the macaque wrist was either in a position of radial or ulnar deviation at touch-down. In general, the digitigrade and semi-digitigrade strides entailed slightly radially deviated wrists, while the palmigrade strides entailed overall more ulnar deviation. However, it cannot be ruled out that these are simply inter-individual differences.

Compared with the macaque hand postures, chimpanzee knuckle-walking entailed overall more ulnar deviation at the wrist, as well as a larger range of motion (ROM) of ulnar and radial deviation during stance phase. At touchdown, the chimpanzee wrist was 17.7 deg more ulnarly deviated than that of the macaques (chimpanzees: −12.0±9.2 deg; macaques: 5.7±11.0 deg) and was 25.2 deg more ulnarly deviated at 50% of stance phase (chimpanzees: −17.4±9.2 deg; macaques: 7.8±8.6 deg). The ulnar and radial deviation ROM during stance phase (5–95% stance excluding the portion immediately after touchdown and prior to lift-off) was 9 deg larger for chimpanzees than for macaques (chimpanzees: 20.7±2.9 deg, n=9; macaques: 11.6±7.1 deg, n=10). No macaque strides entailed greater than 20 deg of ulnar deviation at the wrist, whereas most of the chimpanzee strides did.

Supination

During knuckle-walking, the wrist pronated slightly throughout most of stance phase (Fig. 4B). There were some differences between chimpanzee subjects: one subject touched down with a slightly supinated wrist (10.2±3.2 deg), whereas the other had a slightly pronated wrist (−1.0±2.2 deg). It is important to re-emphasize that pronation/supination here refers only to that motion between the forearm and metacarpals (wrist motion) and is not inclusive of pronation/supination of the forearm itself.

All macaque trials largely followed the same pattern during the first half of stance phase. The wrist was slightly supinated at touchdown (touchdown supination angle, 5.4±2.4 deg), and then quickly maximally pronated within the first 30–40% of stance phase

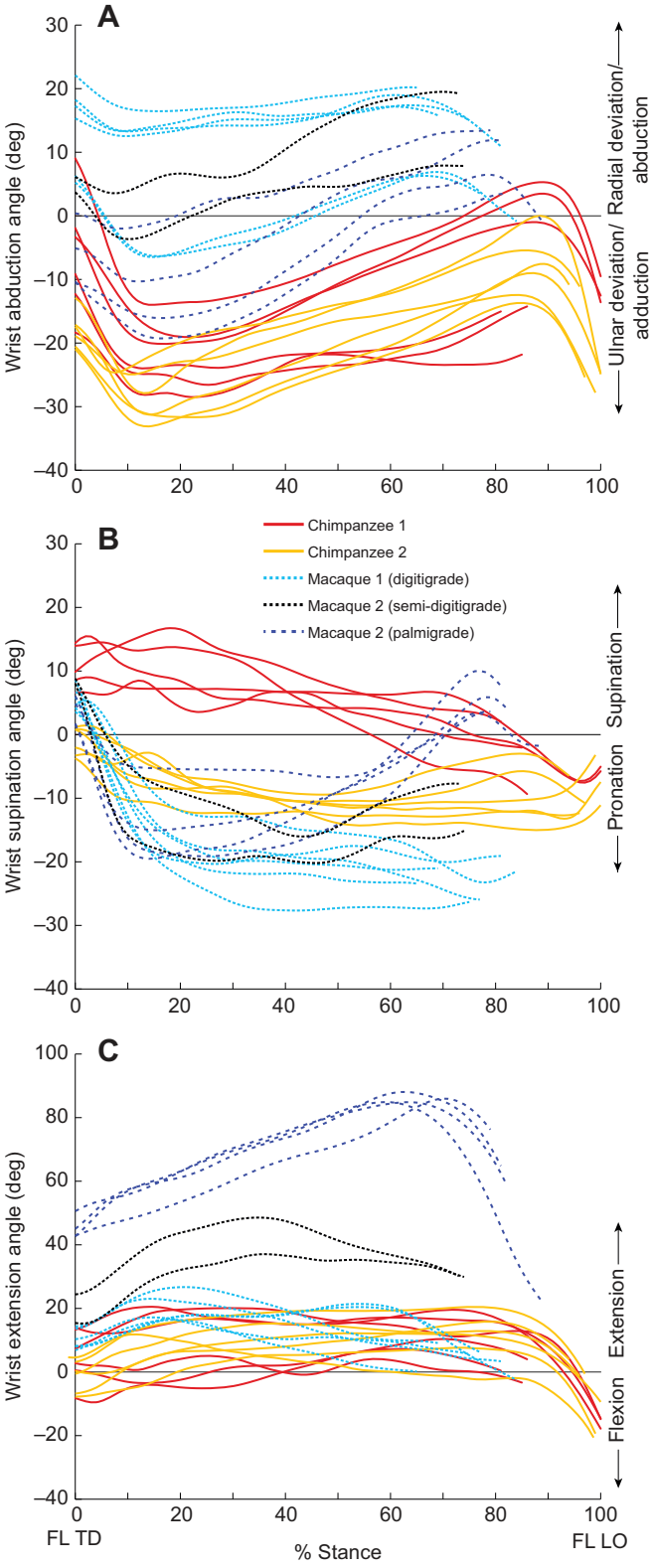

Fig. 4. Three-dimensional kinematics of the wrist. Data are shown for (A) radial deviation/abduction (+) and ulnar deviation/adduction (–), (B) supination (+) and pronation (–), and (C) extension (+) and flexion (–) over 0–100% of stance phase. Chimpanzee knuckle-walking strides are solid red and orange lines; macaque strides are dashed lines: digitigrady (subject 1) is light blue, semi-digitigrady (subject 2) is black, and palmigrady (subject 2) is dark blue with long dashes. Note the difference in y-axis scale for wrist extension. FL TD, forelimb touchdown; FL LO, forelimb lift-off.

Journal of Experimental Biology (2020) 223, jeb224360. doi:10.1242/jeb.224360

Table 1. Three-dimensional kinematic data for the wrist

		Chimpanzee			Macaque			
		Subject 1	Subject 2	Average	Subject 1 (D)	Subject 2 (SD)	Subject 2 (P)	Average
Wrist radial deviation (deg)								
Touchdown	Mean	−6.0	−18.0	−12.0	14.1	4.9	−6.4	5.7
	s.d.	9.5	2.9	9.2	6.8	1.7	5.2	11.0
	n	6	6	12	6	2	4	12
50% stance	Mean	−16.0	−18.8	−17.4	12.0	10.0	0.3	7.8
	s.d.	7.0	4.5	5.8	7.7	7.6	6.2	8.6
	n	6	6	12	6	2	4	12
Minimum (<50% stance)[a]	Mean	−22.0	−28.9	−25.5	7.1	0.0	−11.9	−0.4
	s.d.	5.3	3.6	5.6	10.6	5.1	7.6	12.2
	n	6	6	12	6	2	4	12
Maximum (>50% stance)[a]	Mean	2.6	−8.0	−4.5	14.5	13.7	9.2	13.3
	s.d.	3.2	5.0	6.8	6.2	8.2	3.8	5.9
	n	3	6	9	6	2	2	10
ROM (5–95% stance)[a]	Mean	20.3	20.9	20.7	7.4	13.8	22.4	11.6
	s.d.	2.9	3.2	2.9	4.4	3.1	0.2	7.1
	n	3	6	9	6	2	2	10
Wrist supination (deg)								
Touchdown	Mean	10.2	−1.0	4.6	5.6	8.4	3.5	5.4
	s.d.	3.2	2.2	6.5	1.9	0.5	2.3	2.4
	n	6	6	6	6	2	4	12
Minimum	Mean	−5.4	−12.3	−9.7	−23.1	−18.1	−15.1	−18.9
	s.d.	3.5	2.1	4.4	3.3	2.9	6.0	5.6
	n	3	5	8	4	2	4	10
Maximum	Mean	12.0	−0.9	5.5	5.7	8.4	6.7	6.5
	s.d.	3.9	2.3	7.4	1.8	0.5	2.3	2.0
	n	6	6	12	6	2	4	12
ROM	Mean	15.8	11.0	13.2	28.6	26.5	21.8	25.5
	s.d.	5.6	3.1	4.8	2.9	2.4	7.7	5.8
	n	4	5	9	4	2	4	10
Wrist extension (deg)								
Touchdown	Mean	4.9	−1.5	1.7	10.2	19.9	45.3	23.5
	s.d.	8.4	4.7	7.3	3.1	6.3	3.7	16.8
	n	6	6	12	6	2	4	12
Maximum	Mean	13.8	13.6	13.7	20.9	42.8	85.9	46.2
	s.d.	7.1	4.6	5.7	3.8	8.1	1.5	30.7
	n	6	6	12	6	2	4	12

D, digitigrade; SD, semi-digitigrade; P, palmigrade; *n*, number of strides.

[a]For radial deviation, minimum radial deviation was calculated within the first 50% of stance phase to exclude the ulnar deviation, which occurred immediately prior to lift-off. Similarly, maximum radial deviation was calculated within the final 50% of stance, thus excluding the radial deviation at touchdown, and range of motion was calculated between 5% and 95% of stance phase.

(maximum pronation angle, −18.9±5.6 deg, *n*=10). For palmigrady, the wrist then steadily supinated beginning at approximately 40% of stance phase, whereas the digitigrade strides did not. The semi-digitigrade strides followed an intermediate pattern in this regard.

Overall, the ROM of wrist supination/pronation for chimpanzee knuckle-walking was approximately half that of macaques (chimpanzees: 13.2±4.8 deg, *n*=9; macaques: 25.5±5.8 deg, *n*=10).

Extension

Knuckle-walking in chimpanzees involved relatively little flexion/extension motion over the stance phase (Fig. 4C). Following touchdown, the wrist generally extended throughout stance phase to its maximum extension angle (touchdown extension angle, 1.7±7.3 deg; maximum extension angle, 13.7±5.7 deg). Maximum extension angles ranged between 5.1 and 20.1 deg. Beginning at ∼80% of stance phase, the wrist then flexed 10–20 deg in preparation for swing phase.

Digitigrady in macaques involved wrist extension that was broadly similar to the knuckle-walking pattern, though with slightly more wrist extension (touchdown extension angle: 10.2±3.1 deg; maximum extension angle: 20.9±3.8 deg). Palmigrady entailed wrist extension of 45.3±3.7 deg at touchdown, which steadily increased to a maximum of 86.0±1.5 deg at 60–75% of stance phase. This was followed by more rapid flexion in preparation for lift off. The two semi-digitigrade strides displayed an intermediate pattern of wrist extension (touchdown extension angle: 15.4–24.4 deg; maximum extension angle: 37.1–48.6 deg). The wrist extended by 21.6–24.2 deg during the first ∼40% of stance, at which point wrist extension ceased or began to decrease.

Metacarpophalangeal motion

Extension

MCP joint extension was broadly similar across the second to fifth digits, though with some differences between digits (Fig. 5A–D). For chimpanzee knuckle-walking, the MCP joints were all extended at touchdown (Table 2). One chimpanzee for some strides did not contact the ground with the second and fifth digits, and instead held the MCP joints in flexion. This resulted in negative angles for two and five strides of the second and fifth MCP joints, respectively. These strides were included in Fig. 5, but omitted from the summary statistics described below.

The timing and magnitude of MCP extension during knuckle-walking differed between digits. In general, maximum MCP extension monotonically decreased from digits 2 to 5 during

Journal of Experimental Biology (2020) 223, jeb224360. doi:10.1242/jeb.224360

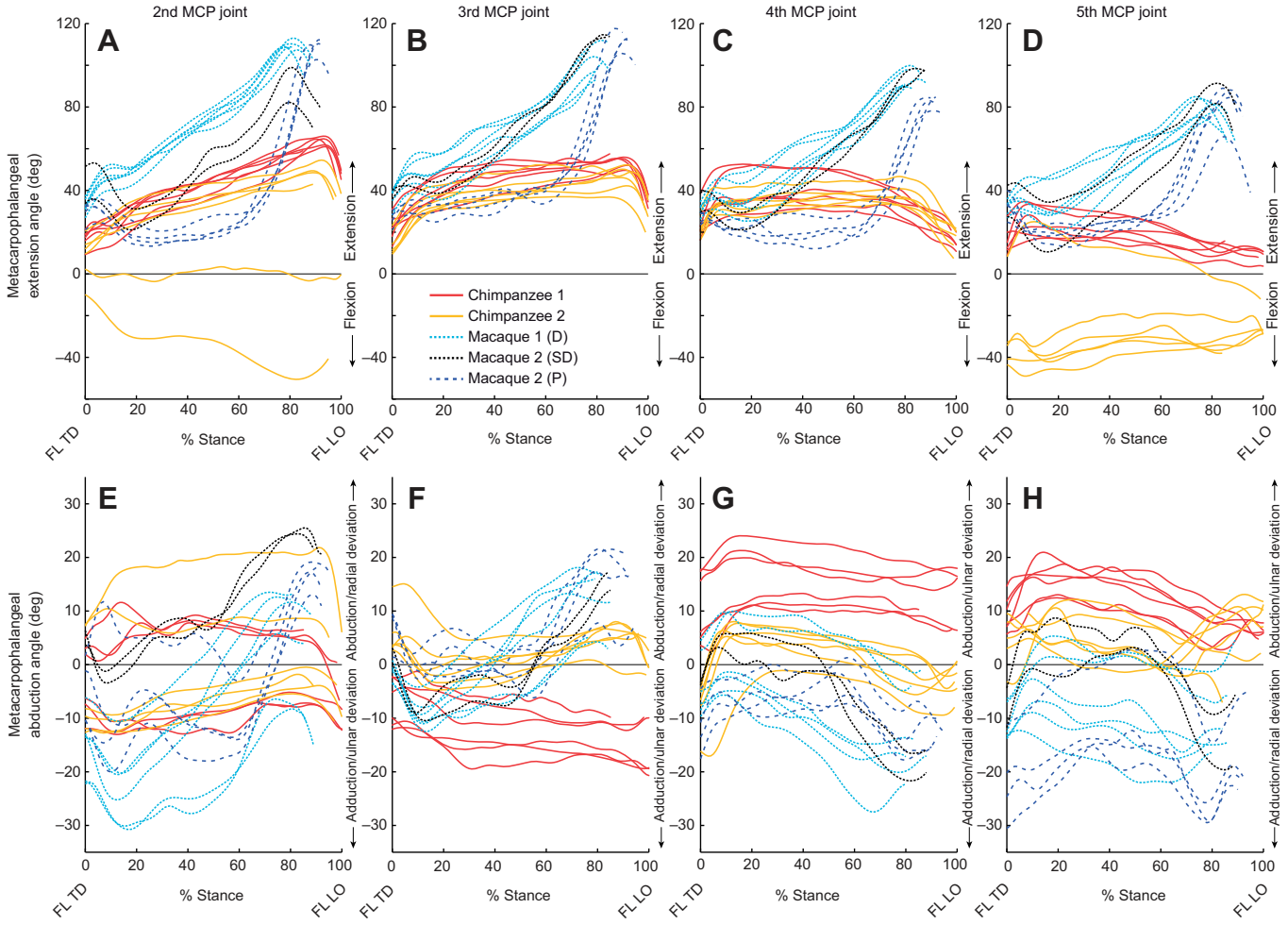

Fig. 5. Three-dimensional metacarpophalangeal (MCP) joint kinematics. Data are shown for the second (A,E), third (B,F), fourth (C,G) and fifth (D,H) MCP joints in (A–D) extension (+) and flexion (–) and (E–H) abduction (+) and adduction (–). Colors and abbreviations follow conventions in Fig. 4. D, SD and P represent digitigrady, semi-digitigrady and palmigrady, respectively. For E–H, abduction is always positive, but given the anatomical coordinate system of the hand, radial deviation is positive for digits two and three (E,F), but negative for digits four and five (G,H). Note the difference in *y*-axis scale between A–D and E–H.

knuckle-walking (MCP 2, 58.8±7.0 deg, *n*=8; MCP 3, 49.9±5.9 deg, *n*=11; MCP 4, 40.4±6.8 deg; MCP 5, 26.0±6.5 deg, *n*=7). Furthermore, the timing of maximum extension differed across the hand (Fig. 5A–D). The second MCP joint displayed maximum extension angles late in stance phase (~90–95%), whereas maximum extension at the fifth MCP joint occurred early (~0–10%). The third and fourth MCP joints had less dramatic increases in joint extension throughout the stance phase, but the third MCP joint generally showed later-occurring maximum extension angles and the fourth MCP joint an earlier maximum.

For macaque digitigrady, the MCP joints were extended at touchdown and steadily increased to the maximum, which occurred between 70 and 90% of stance phase for all digits. During digitigrady, the second and third MCP joints displayed the highest levels of extension (MCP 2, 109.5±2.0 deg; MCP 3, 108.0±5.5 deg, *n*=2). The maximum extension angle then decreased at the fourth MCP joint (MCP 4, 95.2±4.5 deg, *n*=4) and further decreased at the fifth MCP joint (MCP 5, 81.4±4.4 deg, *n*=4).

During palmigrady, the MCP joints were generally as extended as those during digitigrady at touchdown (Table 2). Following touchdown, the joints flexed slightly and then remained largely static until approximately 60% of stance phase. After this point they rapidly extended to their maximum values, which occurred at approximately 85–90% of stance phase (maximum extension angle, MCP 2, 107.6±4.3 deg, *n*=3; MCP 3, 111.7±8.5 deg, *n*=2; MCP 4, 81.9±3.2 deg, *n*=3; MCP 5, 81.9±10.9 deg). Maximum extension angles were similar to those of digitigrady at the second, third and fifth MCP joints, but not at the fourth MCP joint.

The two semi-digitigrade strides generally followed a pattern of motion similar to the digitigrade strides at all but the second MCP joints. At the second digit, the MCP joint showed an intermediate pattern of extension between digitigrady and palmigrady, with maximum joint extension angles that were lower than either digitigrady or palmigrady (82.2–98.9 deg).

Abduction

MCP abduction was more variable than MCP extension, but some trends were present in the data. For chimpanzees (excluding those strides where the second and fifth digits joints were not touching the ground), many of the strides displayed an initial amount of ulnar deviation within the first 15% of stance, followed by a slight and steady degree of radial deviation throughout the remainder of stance. However, not all individual strides displayed this pattern, and some strides displayed little to no motion over stance phase. ROMs were not dramatically different between digits (7.6–12.1 deg; Table 3).

Journal of Experimental Biology (2020) 223, jeb224360. doi:10.1242/jeb.224360

Table 2. Motion of the metacarpophalangeal joints in extension and flexion

		Chimpanzee			Macaque			
		Subject 1	Subject 2	Average	Subject 1 (D)	Subject 2 (SD)	Subject 2 (P)	Average
MCP 2 extension (deg)								
Touchdown	Mean	17.0	14.1	15.8	32.5	42.5	28.8	32.9
	s.d.	4.1	4.7	4.4	3.7	12.6	5.3	7.2
	n	6	4[a]	10	6	2	4	12
Maximum	Mean	63.6	50.9	58.8	109.5	90.6	107.6	105.5
	s.d.	2.1	3.2	7.0	2.0	11.8	4.3	8.7
	n	5	3[a]	8	6	2	3	11
MCP 3 extension (deg)								
Touchdown	Mean	22.1	14.9	18.5	36.6	38.0	26.3	33.4
	s.d.	6.2	5.7	6.8	4.5	3.0	4.1	6.5
	n	6	6	12	6	2	4	12
Maximum	Mean	53.7	46.7	49.9	108.0	114.7	111.7	110.8
	s.d.	2.6	6.1	5.9	5.5	–	8.5	5.8
	n	5	6	11	2	1	2	5
MCP 4 extension (deg)								
Touchdown	Mean	24.8	21.0	22.9	30.6	34.2	26.6	29.9
	s.d.	8.0	4.0	6.3	2.9	6.5	2.8	4.2
	n	6	6	12	6	2	4	12
Maximum	Mean	41.8	38.9	40.4	95.2	98.4	81.9	90.6
	s.d.	8.7	4.5	6.8	4.5	–	3.2	8.1
	n	6	6	12	4	1	3	8
MCP 5 extension (deg)								
Touchdown	Mean	16.0	8.2	14.9	31.8	34.9	32.8	32.6
	s.d.	6.9	–	6.9	3.3	10.6	6.2	5.2
	n	6	1[a]	7	6	2	4	12
Maximum	Mean	26.2	25.0	26.0	81.4	86.5	81.9	82.6
	s.d.	7.1	–	6.5	4.4	6.8	10.9	7.5
	n	6	1[a]	7	4	2	4	10

D, digitigrade; SD, semi-digitigrade; P, palmigrade; *n*, number of strides.
[a]Summary statistics exclude those strides where the MCP joint was held in flexion and not touching the ground (two strides for MCP 2 and five strides for MCP 4).

For all macaque hand postures, the MCP joints tended to be ulnarly deviated early in stance phase, and generally moved into a more radially deviated position later in stance phase. However, the magnitude of the abduction ROM differed between joints, and the fifth MCP joint only seemed to show this pattern of motion for the digitigrade strides. At the fifth MCP joint, the palmigrade and semi-digitigrade strides showed a more parabolic pattern of motion, with the MCP joint being more radially deviated early and late in stance phase, and more ulnarly deviated at midstance. In general, abduction ROMs decreased from the second to the fifth MCP joint (MCP 2, 27.5±4.0 deg, n=11; MCP 3, 19.9±4.3 deg, n=9; MCP 4, 15.9±5.3 deg, n=11; MCP 5, 14.1±4.6 deg, n=11).

Compared with macaques, chimpanzees displayed smaller ROMs in abduction (chimpanzees: 7.6–12.1 deg; macaques: 14.1–27.5 deg). Macaques and chimpanzees largely overlapped in abduction joint position, though macaques tended to use more ulnar deviation at the second MCP joint, and more radial deviation at the third, fourth and fifth MCP joints. In general, this represents the less splayed MCP joint positions of macaques as compared with chimpanzees.

Hand orientation

Hand orientations over the stride are shown in Fig. 6. For all figures, the orientation of the normal vector for a plane fit to the metacarpals is projected outward from the palm of the hand (black dot in Figs 3 and 6). The arrows represent the orientation of this vector at 50% of stance phase, while the pathways represent the endpoint of the vector at each frame over stance phase, beginning at touchdown (open colored circles). Thus the orientation of the hand at any given point is the vector connecting the black dot with a point on the colored lines.

The chimpanzee knuckle-walking strides analyzed here generally entailed the palm being oriented more medially than posteriorly (Fig. 6A,B). At touchdown, the palm orientation in the coronal plane (PA_c; Fig. 6B) was 11.4±10.2 deg, which increased slightly to 18.6±13.9 deg at 50% of stance phase (Table 4). Palm orientation at 50% of stance phase in the coronal plane ranged from −1.1 to 41.3 deg. In the sagittal plane, the chimpanzee palm varied between being pointed slightly upward and slightly downward at midstance (Fig. 6C).

The orientation of the macaque hand generally followed a more regular pattern than that of the chimpanzees (Fig. 6). At 50% of stance, the palm was oriented nearly directly down (PA_s=86.2±2.0 deg; Fig. 6C) and slightly medially (PA_c=18.6±10.9 deg; Fig. 6B) during palmigrady. During digitigrady, the palm faced largely posteriorly and inferiorly (PA_s=23.9±3.4 deg; Fig. 6C) as well as slightly medially (PA_c=71.5±3.9 deg; Fig. 6B). The two semi-digitigrade strides were largely intermediate between digitigrady and palmigrady (PA_s=43.2–49.4 deg; PA_c=67.8–71.0 deg).

DICUSSION

The unusual knuckle-walking hand posture of chimpanzees, bonobos and gorillas has played a considerable role in the interpretations of human origins. Evaluating the origin of knuckle-walking, as well as assessing whether knuckle-walking preceded bipedalism, relies on evaluation of form–function inferences largely based on bony morphology. However, these inferences have largely relied on incomplete or non-existent quantitative descriptions of knuckle-walking in chimpanzees, as well as comparative data on other quadrupedal monkeys.

The data herein are the first detailed, 3-D data of chimpanzee knuckle-walking and macaque digitigrady/palmigrady. These data

Journal of Experimental Biology (2020) 223, jeb224360. doi:10.1242/jeb.224360

Table 3. Motion of the metacarpophalangeal joints in abduction and adduction

		Chimpanzee			Macaque			
		Subject 1	Subject 2	Average	Subject 1 (D)	Subject 2 (SD)	Subject 2 (P)	Average
MCP 2 abduction (deg)								
Touchdown	Mean	−2.6	−10.6	−5.8	−15.0	5.0	−5.1	−8.4
	s.d.	6.8	2.1	6.6	6.1	1.9	6.2	9.4
	n	6	4[a]	10	6	2	4	12
Maximum	Mean	1.5	−2.9	−0.2	4.8	25.0	16.5	11.7
	s.d.	8.6	2.2	6.9	9.8	0.8	3.1	11.0
	n	6	4[a]	10	6	2	3	11
Minimum	Mean	−8.4	−11.3	−9.9	−22.9	−2.3	−12.9	−16.1
	s.d.	8.9	1.6	6.1	7.5	1.5	7.1	10.2
	n	4	4[a]	8	6	2	4	12
ROM	Mean	6.7	8.5	7.6	27.7	27.3	27.0	27.5
	s.d.	0.6	0.8	1.1	2.8	2.3	4.6	4.0
	n	4	4[a]	8	6	2	3	11
MCP 3 abduction (deg)								
Touchdown	Mean	−7.2	5.6	−0.8	−1.5	1.7	7.2	2.0
	s.d.	4.5	4.5	7.9	1.7	1.9	3.9	4.7
	n	6	6	12	6	2	4	12
Maximum	Mean	−6.7	8.0	0.0	11.5	–	17.1	14.0
	s.d.	4.6	4.3	8.8	6.6	–	6.5	6.8
	n	6	5	11	5	0	4	9
Minimum	Mean	−16.6	−0.9	−8.1	−9.3	−9.7	−2.1	−6.9
	s.d.	4.4	3.3	9.0	2.9	1.0	3.4	4.5
	n	5	6	11	6	2	4	12
ROM	Mean	8.9	8.8	8.8	20.5	–	19.1	19.9
	s.d.	0.5	3.0	2.0	4.0	–	5.2	4.3
	n	5	5	10	5	0	4	9
MCP 4 abduction (deg)								
Touchdown	Mean	10.9	−7.3	1.8	−3.9	−3.6	−11.6	−6.4
	s.d.	6.7	4.5	11.0	6.0	0.3	5.5	6.3
	n	6	6	12	6	2	4	12
Maximum	Mean	16.9	5.4	11.1	0.9	4.6	−2.8	0.3
	s.d.	5.6	3.3	7.4	7.1	1.9	3.4	5.8
	n	6	6	12	6	2	4	12
Minimum	Mean	10.1	−7.6	1.2	−14.4	−19.1	−15.9	−15.7
	s.d.	6.2	4.9	10.6	9.7	3.6	1.9	7.2
	n	6	6	12	6	2	3	11
ROM	Mean	6.8	12.9	9.9	15.3	23.7	11.7	15.9
	s.d.	1.4	1.8	3.5	3.5	5.5	2.8	5.3
	n	6	6	12	6	2	3	11
MCP 5 abduction (deg)								
Touchdown	Mean	9.6	−3.1	7.8	−11.1	−8.0	−21.7	−14.1
	s.d.	3.4	–	5.7	3.4	5.2	8.1	7.6
	n	6	1[a]	7	6	2	4	12
Maximum	Mean	16.7	12.1	16.1	−5.1	5.9	−9.7	−4.7
	s.d.	3.3	–	3.5	6.8	3.9	8.4	8.6
	n	6	1[a]	7	5	2	4	11
Minimum	Mean	4.6	−3.6	3.0	−14.2	−14.5	−25.1	−17.8
	s.d.	2.2	–	4.2	6.0	7.3	7.4	8.0
	n	4	1[a]	5	6	2	4	12
ROM	Mean	11.2	15.8	12.1	10.5	20.4	15.4	14.1
	s.d.	1.8	–	2.6	2.4	3.4	2.9	4.6
	n	4	1[a]	5	5	2	4	11

D, digitigrade; SD, semi-digitigrade; P, palmigrade; *n*, number of strides.
[a]Summary statistics exclude those strides where the MCP joint was held in flexion and not touching the ground (two strides for MCP 2 and five strides for MCP 4).

demonstrate that knuckle-walking is characterized by complex non-sagittal plane motion. In particular, these data highlight the distinct use of wrist adduction during knuckle-walking in chimpanzees compared with macaques. These results also highlight digit-level differences in MCP joint posture across the hand in both chimpanzees and macaques. Most importantly, these data provide a complete, 3-D quantification of hand and wrist motion that improves the ability to infer function from skeletal morphology.

Limitations

There are some limitations to the 3-D kinematic data herein that must be considered when interpreting these results. Methodologically, there is always the possibility that skin-based markers may exaggerate, or underestimate, underlying bony motion (Leardini et al., 2005). The marker set used here had a dense sampling of markers (i.e. six to seven for the forearm and eight for the hand), which should minimize this effect. Second, all the elements herein are modeled as rigid bodies, yet some intra-segment motion does occur. This is likely most relevant for the hand segment, for which motion was calculated via all eight MC markers. Motion of the MCs relative to one another was therefore registered as a change in overall segment orientation. The effect of this was likely greatest for wrist supination, where the ROMs recorded here were quite high given the expected amount of wrist supination

Journal of Experimental Biology (2020) 223, jeb224360. doi:10.1242/jeb.224360

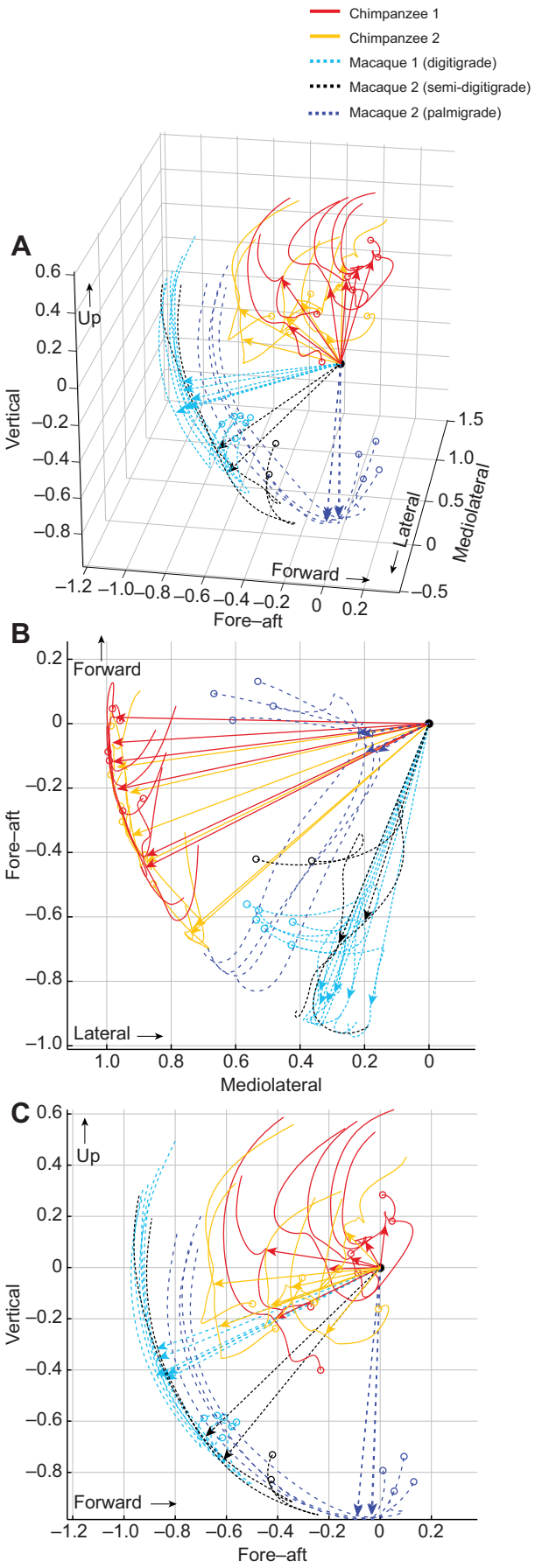

Fig. 6. Orientation of the hand in the global coordinate system. Data are shown in (A) 3-D, (B) the coronal plane and (C) the sagittal plane. All normal vectors are oriented as pointing away from the palm of a right hand (black dot). For each stance phase, the arrows represent the orientation of the metacarpal plane at 50% of stance phase. The open circle represents the orientation of the normal vector at touchdown. The curve represents the path created by the endpoints of the normal vector each instance during stance phase. These vectors and curves were then projected on the (B) coronal and (C) sagittal plane in order to measure coronal palm angle (PA_c, B) and sagittal palm angle (PA_s, C) angles, respectively. Colors follow those in Fig. 4. Up, lateral and forward refer to the global coordinate system.

possible across the radiocarpal and carpal joints. For this reason, the wrist pronation/supination data (between forearm and metacarpals) should be interpreted with some caution. Similarly, given that two line segments were used to calculate MCP motion, MCP joint motion could be resolved into extension and abduction. Rotation of the phalanges would therefore have registered as abduction and/or flexion. Based on observation of the video, this effect is likely minimal (Movie 1). Ultimately, the limitations herein are inherent to all skin-based marker kinematics, and given that the limitations are similar for both species, they are unlikely to dramatically alter the conclusions reached herein.

It is also worth noting that the speeds of the macaques were, non-dimensionally, much faster than those of the chimpanzees. Speed effects on hand and wrist kinematics have been well documented for monkeys, including macaques (Courtine et al., 2005; Patel, 2009; Patel, 2010a; Patel and Polk, 2010), and likely influence chimpanzee kinematics as well. In contrast, all subjects walked at self-selected, and nearly absolutely matched, speeds. Comparisons at self-selected (i.e. preferred speeds) may also be relevant, as they potentially compare mechanical and evolutionary equivalent aspects of locomotion (Hoyt and Taylor, 1981; Irschick, 2000; Perry et al., 1988). However, when interpreting the conclusions below, it is best to keep in mind that speed may be a confounding factor. It is also worth recognizing that the data, though the first of its kind, entail relatively small sample sizes, particularly when dividing by hand posture within macaques. The macaque strides were quite consistent; however, owing to sample size limitations, the discussion largely focuses on the most obvious difference between chimpanzees and macaques, and deemphasizes differences between macaque hand postures.

Finally, because markers had to be visible to the cameras, all chimpanzee steps analyzed were those where the hand was placed outside (lateral to) the ipsilateral foot during over-striding. The outside limbs tend to have slightly lower peak forces and pressures than the inside limbs, though this effect is minor and non-significant at the forelimb, if present at all (Demes et al., 1994; Reynolds, 1985; Wunderlich and Jungers, 2009). Nevertheless, there are likely differences in hand placement between inside and outside limbs that could not be captured here. The extent to which these may affect MCP and wrist joint angles is unknown.

Wrist motion

The data presented herein allow – for the first time – accurate quantification of wrist ulnar and radial deviation (adduction and abduction) during knuckle-walking. And, indeed, a larger range of wrist ulnar deviation was one of the most notable differences between chimpanzees and macaques. Knuckle-walking entailed, on average, 14 and 32 deg greater ulnar deviation than digitigrady and palmigrady, respectively (Fig. 4A). Furthermore, the high wrist ulnar deviation took place while the hand was in a semi-pronated position (Fig. 6B). The overall pattern of motion accords well with

Journal of Experimental Biology (2020) 223, jeb224360. doi:10.1242/jeb.224360

Table 4. Orientation of the hand at touchdown and 50% of stance phase

		Chimpanzee			Macaque			
		Subject 1	Subject 2	Average	Subject 1 (D)	Subject 2 (SD)	Subject 2 (P)	Average
Coronal palm angle (PA_c) (deg)								
Touchdown	Mean	6.5	16.2	11.4	51.0	43.8	−7.3	30.4
	s.d.	7.6	10.7	10.2	5.0	8.1	5.3	28.4
	n	6	6	12	6	2	4	12
50% stance	Mean	12.3	25.0	18.6	71.5	69.4	18.6	53.5
	s.d	11.6	13.9	13.9	3.9	2.3	10.9	28.4
	n	6	6	12	6	2	4	12
Sagittal palm angle (PA_s) (deg)								
Touchdown	Mean	−19.9	28.7	4.4	44.7	61.4	95.1	64.3
	s.d	66.7	30.9	55.7	2.9	1.9	3.6	23.8
	n	6	6	12	6	2	4	12
50% stance	Mean	−25.6	9.9	−7.8	23.9	46.3	86.2	48.4
	s.d.	44.1	31.5	41.0	3.1	4.4	1.9	29.3
	n	6	6	12	6	2	4	12

D, digitigrade; SD, semi-digitigrade; P, palmigrade; *n*, number of strides.

the description of Jenkins and Fleagle (1975) of ulnar deviation at touchdown, and the wrist maintaining an ulnarly deviated position during stance. However, peak wrist ulnar deviation was generally at the high end, or higher, than that reported by Jenkins and Fleagle (1975) (their −10 to −20 deg of ulnar deviation versus −25.5± 5.6 deg of ulnar deviation herein).

The range of maximum wrist extension measured here was approximately 5–20 deg. This is in agreement with the previous cineradiographic observations (10–15 deg; Jenkins and Fleagle, 1975). However, extension angles are much higher than those reported in other previous 2-D studies. In a study of zoo chimpanzees, Finestone et al. (2018) reported largely flexed wrists in chimpanzees during stance phase (touchdown: −13.8± 5.9 deg; midstance: −8.1±8.5 deg). Similarly, Pontzer et al. (2014) reported approximately 20 deg of wrist flexion for most of stance phase. The out-of-plane nature of the knuckle-walking hand may account for some of this discrepancy. The hand orientations measured here involved the palm being oriented medially to some degree. Given this, it is likely that 2-D sagittal measurements of wrist motion are measuring, to a large extent, wrist ulnar/radial deviation in addition to flexion/extension. Measuring the 2-D angle of an ulnarly deviated and slightly extended wrist projected onto a sagittal plane would likely register flexion, perhaps explaining the lack of wrist extension in previous 2-D studies (Finestone et al., 2018; Pontzer et al., 2014). However, it is also expected that over more varied substrate types such as the zoo enclosures of Finestone et al. (2018), hand postures will be more varied, including more flexed wrist positions during stance phase (e.g. their fig. 1C). Nevertheless, similar to previous 2-D studies (Finestone et al., 2018; Pontzer et al., 2014), the range of motion of wrist extension over stance phase herein was quite limited, only 12 deg between touchdown and maximum extension.

The extension angles measured here also bear on the idea that chimpanzees display more extended wrists, while gorillas have wrists that are more ‘columnar’ (Kivell and Schmitt, 2009). This suggestion, based on carpal morphology, has been widely adopted in the human evolution literature (e.g. Le Maître et al., 2017; Macho et al., 2010; Saunders et al., 2016; Schilling et al., 2014; Simpson et al., 2018; Thorpe et al., 2014). The data herein show that the chimpanzee wrist is only slightly extended. Indeed, some strides fluctuated around the neutral position for most of stance phase (Fig. 4B). Thus, though slightly extended, the chimpanzee wrist could largely be argued to be columnar in the first place. This does not leave much room for gorilla wrists to be more columnar than those of chimpanzees. That chimpanzees and gorillas have similar wrist extension was also supported by the 2-D zoo-based study of Finestone et al. (2018), who found little-to-no difference in wrist joint angles. Together, these available kinematic data suggest that there is little evidence that African apes differ in habitual wrist extension during knuckle-walking.

For macaques, wrist extension angles measured here largely overlap with previous 2-D measures at similar speeds during digitigrady (Courtine et al., 2005; Patel, 2009) and palmigrady (Patel, 2010a). Compared with chimpanzees, extension during digitigrady in macaques nearly entirely overlapped the range of extension used during knuckle-walking (though digitigrady did entail somewhat higher maximum extension values). In evaluating proposed morphology associated with knuckle-walking, it has been previously recognized that the ‘vertical manus’ hand postures (digitigrady and knuckle-walking; Orr, 2005; Schmitt et al., 2016) may result in similar wrist biomechanics (Dainton, 2001; Orr, 2005; Patel, 2010b; Patel and Carlson, 2007; Sarmiento, 1988). These data offer support for such interpretations, highlighting the complexities associated with discriminating digitigrade and knuckle-walking hand and wrist morphologies in terrestrial primates.

Metacarpophalangeal joint motion

Metacarpophalangeal joint motion showed distinct trends across the hand. In general, maximum extension angles decreased across the metacarpal row in both chimpanzees and macaques from digit two to five. In chimpanzees, the timing of maximum extension also shifted earlier from the second MCP joint (late in stance) to the fifth (early in stance). The trends in chimpanzees nearly perfectly reflect the differences in peak pressure magnitude and timing across the digits. Both peak digital pressures and timing of peak pressure decrease monotonically from digit two (~80 N cm^{-2} at ~62% of stance phase) to digit five (~20 N cm^{-2} at 10% of stance phase; Wunderlich and Jungers, 2009). This may also be true of macaque digital pressures, but current palmar pressure distributions for monkeys are limited, and none have yet resolved digital level differences within the hand (Higurashi et al., 2017; Patel and Wunderlich, 2010).

Compared with oft-utilized diagrammatic portrayals of the MCP joint in knuckle-walking (Kivell and Schmitt, 2009; Richmond and Strait, 2000; Susman, 1979) the results herein indicate that the MCP joints are, in actuality, much more extended than generally considered. For instance, Susman (1979) illustrated MCP extension

of approximately 21 deg compared with the 26–59 deg measured here (Table 2). The higher MCP extension angles do, however, match some previous videographic descriptions (e.g. fig. 2 of Tuttle, 1967). For macaques, the results reported here can be compared with those of previous 2-D studies reporting lateral-view metacarpal–ground angle (MGA; Patel, 2009; Patel, 2010a). The MCP joint angles measured here for digit five are smaller than would be estimated on the basis of MGA. This is largely due to the fact that in macaques, especially during palmigrady, the proximal phalanx is not parallel to the ground. The proximal interphalangeal joint is elevated off of the ground. This therefore decreases MCP joint angle causing it to be smaller than expected on the basis of MGA.

Across all hand postures, it might be expected that digitigrady would exhibit the highest MCP extension angles, followed by knuckle-walking and palmigrady. Interestingly, at most digits, palmigrady and digitigrady actually had similar maximum MCP joint extension. Of course the main difference between digitigrady and palmigrady is that in the latter, MCP extension is rapid, and largely occurs after 60–70% of stance phase. During much of midstance (e.g. 20–60%) MCP joints during palmigrady were as or less extended than those of chimpanzees knuckle-walking.

The large overlap of maximum MCP joint extension angles between digitigrady and palmigrady bears on one of the more debated metacarpal morphologies associated with knuckle-walking, the transverse dorsal ridge of the metacarpal heads. This trait was originally proposed to be a bony stop in chimpanzees and gorillas, preventing excessive hyperextension of the MCP joint (Tuttle, 1967). On the basis of a dorsal ridge, the fossil *Equatorius africanus* was at one point hinted to be a knuckle-walker (McCrossin et al., 1998). However, prominent dorsal ridges are also seen in some large-bodied, terrestrial cercopithecoids (McCrossin and Benefit, 1997; Orr, 2005; Patel and Maiolino, 2016; Richmond et al., 2001). Similar to the wrist, this raised the possibility that 'digitigrade' knuckle walking and digitigrady (*sensu stricto*) might result in similar functional demands and bony morphology. That maximum MCP extension during palmigrady and digitigrady largely overlap further complicates this notion. If the dorsal ridge aids in preventing hyperextension (see Simpson et al., 2018 for an alternative viewpoint), this function would be equally applicable to digitigrady and palmigrady, as both are associated with similar maximum MCP extension. Thus, digitigrady alone may be insufficient to explain the presence of dorsal metacarpal ridges in cercopithecoids, and the presence of a ridge may not discriminate between knuckle-walking and any other hand postures. The overlap in MCP joint extension may also explain why some studies have found little difference in the morphology of the metacarpophalangeal joints between digitigrade and palmigrade primates (Patel, 2010b; Rein and McCarty, 2012). This does, however, assume that the digitigrade and palmigrade data herein are representative of other cercopithecoids, which may not be the case.

Hand orientation

Consistent with previous studies (Matarazzo, 2013; Tuttle, 1967, 1969b; Wunderlich and Jungers, 2009), the chimpanzee subjects in this study largely used a semi-pronated, 'palm-in' hand posture. Palm orientation varied from nearly directly medially (PA_c=−1.1 deg) to almost halfway between medially and posteriorly (PA_c=41.3 deg) at 50% of stance phase. A more medially oriented hand is the most common hand posture for knuckle-walking in chimpanzees (Matarazzo, 2013; Wunderlich and Jungers, 2009), whereas palm-back postures are less frequent (particularly in the chimpanzee subjects here) during terrestrial knuckle-walking (Wunderlich and Jungers, 2009).

These data also show that hand orientation is fairly normally distributed within the range measured here. Chimpanzee hand orientations also appeared to be less stereotypical than macaque hand orientations. The descriptions of knuckle-walking hand postures as 'palm-in' versus 'palm-back', though useful for dichotomizing styles of knuckle-walking of chimpanzees and gorillas (Matarazzo, 2013; Tuttle, 1967), are likely oversimplifications; 'palm-in' and 'palm-back' are simply two ends of a continuous distribution of hand orientation. Further, documentation of hand posture usage in mountain gorillas suggest that knuckle-walking hand orientation variability is much greater in the wild (Thompson et al., 2018a). As such, the terms 'palm-in' and 'palm-back' terms may be of less utility than their presence in the literature would suggest.

Conclusions

The data herein provide the first foundational dataset on 3-D motion of the wrist and hand, and digit-level data on the metacarpophalangeal joints in knuckle-walking chimpanzees and during palmigrady and digitigrady walking in macaques. These data highlight the unique 3-D motions associated with knuckle-walking, including increased amounts of ulnar deviation at the wrist. Perhaps more importantly, however, are the areas of similarity between chimpanzees and macaques, as well as between different hand postures within macaques. Although wrist extension during knuckle-walking was limited, it largely overlapped with that experienced in digitigrade macaques. More surprisingly, the maximum metacarpophalangeal joint extension angles were nearly the same during digitigrady and palmigrady within macaques. Both findings further emphasize the complexities associated with identifying specific morphological adaptions associated with knuckle-walking. In particular, these data raise questions about morphologies at the metacarpophalangeal joints, which are thought to help in limiting extension during knuckle-walking and digitigrady. Most importantly, however, this dataset forms the basis from which future evaluation of musculoskeletal adaptations for knuckle-walking can be tested.

Acknowledgements

I thank B. Demes and N. Holowka for their help with chimpanzee data collection, J. Young and A. Foster for their facilitation and help with macaque data collection, K. Lasek for her invaluable chimpanzee training, and B. Demes, S. Larson, S. Almécija, T. Kivell and C. Orr for comments and feedback on earlier versions of this work.

Competing interests

The author declares no competing or financial interests.

Funding

This research was supported by National Science Foundation grants SMA-1719432, BCS-0935321 and BCS-1126790.

Supplementary information

Supplementary information available online at
https://jeb.biologists.org/lookup/doi/10.1242/jeb.224360.supplemental

References

Alexander, R. M. and Jayes, A. S. (1983). A dynamic similarity hypothesis for the gaits of quadrupedal mammals. *J. Zool.* **201**, 135-152. doi:10.1111/j.1469-7998.1983.tb04266.x

Barak, M. M., Sherratt, E. and Lieberman, D. E. (2017). Using principal trabecular orientation to differentiate joint loading orientation in the 3rd metacarpal heads of humans and chimpanzees. *J. Hum. Evol.* **113**, 173-182. doi:10.1016/j.jhevol.2017.08.018

Begun, D. R. (2010). Miocene hominids and the origins of the African apes and humans. *Annu. Rev. Anthropol.* **39**, 67-84. doi:10.1146/annurev.anthro.012809.105047

Begun, D. R. and Kivell, T. L. (2011). Knuckle-walking in *Sivapithecus*? The combined effects of homology and homoplasy with possible implications for pongine dispersals. *J. Hum. Evol.* **60**, 158-170. doi:10.1016/j.jhevol.2010.10.002

Chirchir, H., Zeininger, A., Nakatsukasa, M., Ketcham, R. A. and Richmond, B. G. (2017). Does trabecular bone structure within the metacarpal heads of primates vary with hand posture? *Comptes Rendus Palevol* **16**, 533-544. doi:10.1016/j.crpv.2016.10.002

Courtine, G., Roy, R. R., Hodgson, J., McKay, H., Raven, J., Zhong, H., Yang, H., Tuszynski, M. H. and Edgerton, V. R. (2005). Kinematic and EMG determinants in quadrupedal locomotion of a non-human primate (rhesus). *J. Neurophysiol.* **93**, 3127-3145. doi:10.1152/jn.01073.2004

Crompton, R. H., Vereecke, E. E. and Thorpe, S. K. S. (2008). Locomotion and posture from the common hominoid ancestor to fully modern hominins, with special reference to the last common panin/hominin ancestor. *J. Anat.* **212**, 501-543. doi:10.1111/j.1469-7580.2008.00870.x

Dainton, M. (2001). Did our ancestors knuckle-walk? *Nature* **410**, 324-325. doi:10.1038/35066634

Demes, B., Larson, S. G., Stern, J. T., Jungers, W. L., Biknevicius, A. R. and Schmitt, D. (1994). The kinetics of primate quadrupedalism: "hindlimb drive" reconsidered. *J. Hum. Evol.* **26**, 353-374. doi:10.1006/jhev.1994.1023

Doran, D. M. (1997). Ontogeny of locomotion in mountain gorillas and chimpanzees. *J. Hum. Evol.* **32**, 323-344. doi:10.1006/jhev.1996.0095

Dunmore, C. J., Kivell, T. L., Bardo, A. and Skinner, M. M. (2019). Metacarpal trabecular bone varies with distinct hand-positions used in hominid locomotion. *J. Anat.* **235**, 45-66. doi:10.1111/joa.12966

Finestone, E. M., Brown, M. H., Ross, S. R. and Pontzer, H. (2018). Great ape walking kinematics: implications for hominoid evolution. *Am. J. Phys. Anthropol.* **166**, 43-55. doi:10.1002/ajpa.23397

Higurashi, Y., Goto, R. and Kumakura, H. (2017). Intra-individual variation in hand postures during terrestrial locomotion in Japanese macaques (*Macaca fuscata*). *Primates* **59**, 61-68. doi:10.1007/s10329-017-0619-6

Hoyt, D. F. and Taylor, C. R. (1981). Gait and the energetics of locomotion in horses. *Nature* **292**, 239-240. doi:10.1038/292239a0

Inouye, S. E. (1994). Ontogeny of knuckle-walking hand postures in African apes. *J. Hum. Evol.* **26**, 459-485. doi:10.1006/jhev.1994.1028

Irschick, D. J. (2000). Comparative and behavioral analyses of preferred speed: *Anolis* lizards as a model system. *Physiol. Biochem. Zool.* **73**, 428-437. doi:10.1086/317733

Jenkins, F. A. and Fleagle, J. G. (1975). Knuckle-walking and the functional anatomy of the wrists in living apes. In *Primate Functional Morphology and Evolution* (ed. R. H. Tuttle), pp. 213-231. The Hague: Mouton.

Kimura, T. (1985). Bipedal and quadrupedal walking of primates: comparative dynamics. In *Primate Morphophysiology, Locomotor Analyses and Human Bipedalism* (ed. S. Kondo), pp. 81-104. Tokyo: University of Tokyo Press.

Kimura, T., Okada, M. and Ishida, H. (1979). Kinesiological characteristics of primate walking: its significance in human walking. In *Environment, Behavior, and Morphology: Dynamic Interactions in Primates* (ed. M. E. Morbeck, H. Preuschoft and N. Gomberg), pp. 297-311. New York: Gustav Fischer.

Kivell, T. L. and Schmitt, D. (2009). Independent evolution of knuckle-walking in African apes shows that humans did not evolve from a knuckle-walking ancestor. *Proc. Natl. Acad. Sci. U. S. A.* **106**, 14241-14246. doi:10.1073/pnas.0901280106

Kivell, T. L., Barros, A. P. and Smaers, J. B. (2013). Different evolutionary pathways underlie the morphology of wrist bones in hominoids. *BMC Evol. Biol.* **13**, 229. doi:10.1186/1471-2148-13-229

Lazenby, R. A., Skinner, M. M., Hublin, J.-J. and Boesch, C. (2011). Metacarpal trabecular architecture variation in the chimpanzee (*Pan troglodytes*): evidence for locomotion and tool-use? *Am. J. Phys. Anthropol.* **144**, 215-225. doi:10.1002/ajpa.21390

Le Maître, A., Schuetz, P., Vignaud, P. and Brunet, M. (2017). New data about semicircular canal morphology and locomotion in modern hominoids. *J. Anat.* **231**, 95-109. doi:10.1111/joa.12619

Leardini, A., Chiari, L., Della Croce, U. and Cappozzo, A. (2005). Human movement analysis using stereophotogrammetry. Part 3. Soft tissue artifact assessment and compensation. *Gait Posture* **21**, 212-225. doi:10.1016/j.gaitpost.2004.05.002

Li, Y., Crompton, R. H., Wang, W., Savage, R. and Günther, M. M. (2004). Hind limb drive, hind limb steering? Functional differences between fore and hind limbs in chimpanzee quadrupedalism. In *Shaping Primate Evolution. Form, Function and Behavior* (ed. F. Anapol, R. Z. German and N. G. Jablonski), pp. 258-277. Cambridge: Cambridge University Press.

Lovejoy, C. O., Simpson, S. W., White, T. D., Asfaw, B. and Suwa, G. (2009). Careful climbing in the Miocene: the forelimbs of *Ardipithecus ramidus* and humans are primitive. *Science* **326**, 70e1-70; e8. doi:10.1126/science.1175827

Macho, G. A., Spears, R. and Leakey, M. G. (2010). An exploratory study on the combined effects of external and internal morphology on load dissipation in primate capitates: its potential for an understanding of the positional and locomotor repertoire of early hominins. *Folia Primatol.* **81**, 292-304. doi:10.1159/000322631

Matarazzo, S. A. (2013). Manual pressure distribution patterns of knuckle-walking apes. *Am. J. Phys. Anthropol.* **152**, 44-50. doi:10.1002/ajpa.22325

Matarazzo, S. A. (2015). Trabecular architecture of the manual elements reflects locomotor patterns in primates. *PLoS One* **10**, e0120436. doi:10.1371/journal.pone.0120436

McCrossin, M. L. and Benefit, B. R. (1997). On the relationships and adaptations of *Kenyapithecus*, a large-bodied hominoid from the middle Miocene of Eastern Africa. In *Function, Phylogeny, and Fossils: Miocene Hominoid Evolution and Adaptations* (ed. D. R. Begun, C. V. Ward and M. D. Rose), pp. 241-267. New York: Plenum Press.

McCrossin, M. L., Benefit, B. R., Gitau, S. N., Palmer, A. K. and Blue, K. T. (1998). Fossil evidence for the origins of terrestriality among old world higher primates. In *Primate Locomotion: Recent Advances* (ed. E. Strasser, J. G. Fleagle, A. L. Rosenberger and H. M. McHenry), pp. 353-396. New York: Plenum Press.

O'Neill, M. C., Lee, L.-F., Demes, B., Thompson, N. E., Larson, S. G., Stern, J. T. and Umberger, B. R. (2015). Three-dimensional kinematics of the pelvis and hind limbs in chimpanzee (*Pan troglodytes*) and human bipedal walking. *J. Hum. Evol.* **86**, 32-42. doi:10.1016/j.jhevol.2015.05.012

Orr, C. M. (2005). Knuckle-walking anteater: a convergence test of adaptation for purported knuckle-walking features of african hominidae. *Am. J. Phys. Anthropol.* **658**, 639-658. doi:10.1002/ajpa.20192

Orr, C. M. (2016). Functional morphology of the primate hand: recent approaches using biomedical imaging, computer modeling and engineering methods. In *The Evolution of the Primate Hand* (ed. T. L. Kivell, P. Lemelin, B. G. Richmond and D. Schmitt), pp. 227-257. New York: Springer Science+Business Media.

Patel, B. A. (2009). Not so fast: Speed effects on forelimb kinematics in cercopithecine monkeys and implications for digitigrade postures in primates. *Am. J. Phys. Anthropol.* **140**, 92-112. doi:10.1002/ajpa.21039

Patel, B. A. (2010a). The interplay between speed, kinetics, and hand postures during primate terrestrial locomotion. *Am. J. Phys. Anthropol.* **141**, 222-234. doi:10.1002/ajpa.21138

Patel, B. A. (2010b). Functional morphology of cercopithecoid primate metacarpals. *J. Hum. Evol.* **58**, 320-337. doi:10.1016/j.jhevol.2010.01.001

Patel, B. A. and Carlson, K. J. (2007). Bone density spatial patterns in the distal radius reflect habitual hand postures adopted by quadrupedal primates. *J. Hum. Evol.* **52**, 130-141. doi:10.1016/j.jhevol.2006.08.007

Patel, B. A. and Maiolino, S. A. (2016). Morphological diversity in the digital rays of primate hands. In *The Evolution of the Primate Hand* (ed. T. L. Kivell, P. Lemelin, B. G. Richmond and D. Schmitt), pp. 55-100. New York: Springer-Verlag.

Patel, B. A. and Polk, J. D. (2010). Distal forelimb kinematics in *Erythrocebus patas* and *Papio anubis* during walking and galloping. *Int. J. Primatol.* **31**, 191-207. doi:10.1007/s10764-010-9394-6

Patel, B. A. and Wunderlich, R. E. (2010). Dynamic pressure patterns in the hands of olive baboons (*Papio anubis*) during terrestrial locomotion: implications for cercopithecoid primate hand morphology. *Anat. Rec.* **293**, 710-718. doi:10.1002/ar.21128

Perry, A. K., Blickhan, R., Biewener, A. A., Heglund, N. C. and Taylor, C. R. (1988). Preferred speeds in terrestrial vertebrates: are they equivalent? *J. Exp. Biol.* **219**, 207-219.

Pontzer, H., Raichlen, D. A. and Rodman, P. S. (2014). Bipedal and quadrupedal locomotion in chimpanzees. *J. Hum. Evol.* **66**, 64-82. doi:10.1016/j.jhevol.2013.10.002

Rein, T. R. and McCarty, L. A. (2012). Metacarpophalangeal joint orientation in anthropoid manual phalanges. *Anat. Rec.* **295**, 2057-2068. doi:10.1002/ar.22600

Reynolds, T. R. (1985). Stresses on the limbs of quadrupedal primates. *Am. J. Phys. Anthropol.* **67**, 351-362. doi:10.1002/ajpa.1330670407

Richmond, B. G. and Strait, D. S. (2000). Evidence that humans evolved from a knuckle-walking ancestor. *Nature* **404**, 382-385. doi:10.1038/35006045

Richmond, B. G., Begun, D. R. and Strait, D. S. (2001). Origin of human bipedalism: the knuckle-walking hypothesis revisited. *Am. J. Phys. Anthropol.* **116**, 70-105. doi:10.1002/ajpa.10019

Sarmiento, E. E. (1988). Anatomy of the hominoid wrist joint: its evolutionary and functional implications. *Int. J. Primatol.* **9**, 281-345. doi:10.1007/BF02737381

Saunders, E. L. R., Roberts, A. M. and Thorpe, S. K. S. (2016). Positional behavior. In *The International Encyclopedia of Biological Anthropology* (ed. A. Fuentes), pp. 1-14. John Wiley & Sons, Inc.

Sayers, K., Raghanti, M. A. and Lovejoy, C. O. (2012). Human evolution and the chimpanzee referential doctrine. *Annu. Rev. Anthropol.* **41**, 119-138. doi:10.1146/annurev-anthro-092611-145815

Schilling, A.-M., Tofanelli, S., Hublin, J. J. and Kivell, T. L. (2014). Trabecular bone structure in the primate wrist. *J. Morphol.* **275**, 572-585. doi:10.1002/jmor.20238

Schmitt, D., Zeininger, A. and Granatosky, M. C. (2016). Patterns, variability, and flexibility of hand posture during locomotion in primates. In *The Evolution of the Primate Hand* (ed. T. L. Kivell), pp. 345-369. New York: Springer Science+Business Media.

Simpson, S. W., Latimer, B. and Lovejoy, C. O. (2018). Why do knuckle-walking African apes knuckle-walk? *Anat. Rec.* **301**, 496-514. doi:10.1002/ar.23743

Smith, R. J. (2018). The continuing misuse of null hypothesis significance testing in biological anthropology. *Am. J. Phys. Anthropol.* **166**, 236-245. doi:10.1002/ajpa.23399

Sockol, M. D., Raichlen, D. A. and Pontzer, H. (2007). Chimpanzee locomotor energetics and the origin of human bipedalism. *Proc. Natl. Acad. Sci. U. S. A.* **104**, 12265-12269. doi:10.1073/pnas.0703267104

Susman, R. L. (1979). Comparative and functional morphology of hominoid fingers. *Am. J. Phys. Anthropol.* **50**, 215-236. doi:10.1002/ajpa.1330500211
Thompson, N. E., Demes, B., O'Neill, M. C., Holowka, N. B. and Larson, S. G. (2015). Surprising trunk rotational capabilities in chimpanzees and implications for bipedal walking proficiency in early hominins. *Nat. Commun.* **6**, 8416. doi:10.1038/ncomms9416
Thompson, N. E., Ostrofsky, K. R., McFarlin, S. C., Robbins, M. M., Stoinski, T. S. and Almécija, S. (2018a). Unexpected terrestrial hand posture diversity in wild mountain gorillas. *Am. J. Phys. Anthropol.* **166**, 84-94. doi:10.1002/ajpa.23404
Thompson, N. E., Rubinstein, D. and Larson, S. G. (2018b). Great ape thorax and shoulder configuration – an adaptation for arboreality or knuckle-walking? *J. Hum. Evol.* **125**, 15-26. doi:10.1016/j.jhevol.2018.09.005
Thompson, N. E., Demes, B., Holowka, N. B. and O'Neill, M. C. (2018c). Step width and frontal plane trunk motion in bipedal chimpanzee and human walking. *J. Hum. Evol.* **125**, 27-37. doi:10.1016/j.jhevol.2018.09.006
Thorpe, S. K. S., McClymont, J. M. and Crompton, R. H. (2014). The arboreal origins of human bipedalism. *Antiquity* **88**, 906-926. doi:10.1017/S0003598X00050778
Tsegai, Z. J., Kivell, T. L., Gross, T., Nguyen, N. H., Pahr, D. H., Smaers, J. B. and Skinner, M. M. (2013). Trabecular bone structure correlates with hand posture and use in hominoids. *PLoS One* **8**, e78781. doi:10.1371/journal.pone.0078781
Tuttle, R. H. (1967). Knuckle-walking and the evolution of hominoid hands. *Am. J. Phys. Anthropol.* **26**, 171-206. doi:10.1002/ajpa.1330260207
Tuttle, R. H. (1969a). Quantitative and functional studies on the hands of the Anthropoidea. I. the Hominoidea. *J. Morphol.* **128**, 309-363. doi:10.1002/jmor.1051280304
Tuttle, R. H. (1969b). Knuckle-walking and the problem of human origins. *Science* **166**, 953-961. doi:10.1126/science.166.3908.953
Tuttle, R. H. (1970). Postural, propulsive, and prehensile capabilities in the cheiridia of chimpanzees and other great apes. In *The Chimpanzee* (ed. H. Bourne), pp. 167-253. Basel: Karger.
Williams, S. A. (2010). Morphological integration and the evolution of knuckle-walking. *J. Hum. Evol.* **58**, 432-440. doi:10.1016/j.jhevol.2010.03.005
Wu, G., van der Helm, F. C. T., Veeger, H. E. J. D., Makhsous, M., Roy, P. V., Anglin, C., Nagels, J., Karduna, A. R., McQuade, K., Wang, X. et al. (2005). ISB recommendation on definitions of joint coordinate systems of various joints for the reporting of human joint motion – part II: shoulder, elbow, wrist and hand. *J. Biomech.* **38**, 981-992. doi:10.1016/j.jbiomech.2004.05.042
Wunderlich, R. E., Jungers, W. L. (2009). Manual digital pressures during knuckle-walking in chimpanzees (*Pan troglodytes*). *Am. J. Phys. Anthropol.* **139**, 394-403. doi:10.1002/ajpa.20994
Zeininger, A., Richmond, B. G. and Hartman, G. (2011). Metacarpal head biomechanics: a comparative backscattered electron image analysis of trabecular bone mineral density in *Pan troglodytes*, *Pongo pygmaeus*, and *Homo sapiens*. *J. Hum. Evol.* **60**, 703-710. doi:10.1016/j.jhevol.2011.01.002